



Pd-supporting LaCoO₃ catalyst with structured configuration for water gas shift reaction

Ryo Watanabe^a, Yusuke Fujita^a, Tomohiro Tagawa^a, Kazumasa Yamamoto^a, Takeshi Furusawa^b, Choji Fukuhara^{a,*}

^a Department of Applied Chemistry and Biochemical Engineering, Graduate School of Engineering, Shizuoka University, 3-5-1, Johoku, Naka-ku, Hamamatsu, Shizuoka 432-8561, Japan

^b Department of Applied Chemistry, Faculty of Engineering, Utsunomiya University, Yoto 7-1-2, Utsunomiya 321-8585, Japan



ARTICLE INFO

Article history:

Received 7 November 2013

Received in revised form 14 February 2014

Accepted 1 March 2014

Available online 13 March 2014

Keywords:

Water gas shift reaction

Structured catalyst

Perovskite-type oxide

LaCoO₃

PdCl₂

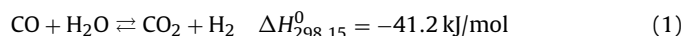
ABSTRACT

The purpose of this study was to develop a structured perovskite-type oxide catalyst for the water gas shift (WGS) reaction, which could make lattice oxygen mobile at a low external heat energy by preparing it as a thin catalyst layer on a metal plate. The thickness of the formed LaCoO₃ layer was about 20 μm, which was confirmed by FE-SEM and EDX analysis. For enhancing its WGS reaction performance, a palladium (Pd) component was supported on the structured catalyst using various Pd precursors. When using a PdCl₂ aqueous solution which was prepared by filtration of the PdCl₂ slurry (the filtration liquid), the Pd-supporting LaCoO₃ structured catalyst showed a high and stable activity. The reason for such an enhanced activity was that the supported Pd was in a highly dispersed state, which was derived from the electrostatic interaction between [PdCl₃(H₂O)]⁻ as the anionic charged precursor in the filtration liquid and the oppositely charged LaCoO₃ support surface confirmed by a UV-vis measurement. In order to remove the remaining chloride ligand from the Pd-supporting LaCoO₃ catalyst surface, a washing treatment was performed by immersing the as-made catalyst in water, NH₃ (aq) or NaOH (aq) at pH 11.5 for 30 min. Consequently, these washing processes were effective for eliminating the remaining chloride ion from the catalyst surface and improving the shift activity of the catalyst. The catalyst washed using NH₃ (aq) showed the highest activity among these catalysts.

© 2014 Elsevier B.V. All rights reserved.

1. Introduction

The fuel cell is one of the attractive technologies in terms of a highly efficient and clean energy resource. Hydrogen for the polymer electrolyte membrane fuel cell (PEMFC) is produced via the steam reforming of hydrocarbons [1,2]. The reformed gas contains not only H₂, but also CO. The CO must be converted below 10 ppm in the reformed gas because CO deactivates the Pt electrodes of fuel cells [3]. The water gas shift (WGS, Eq. (1)) reaction is one of the most effective reactions for CO reducing processes.

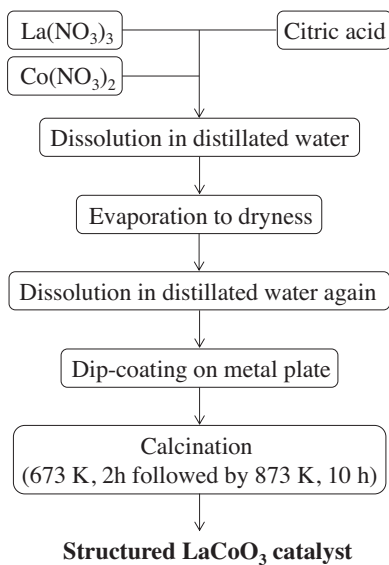


The WGS reaction is an exothermic reaction and the equilibrium conversion is low at high temperature due to thermodynamic limitations. Therefore, the reaction temperature should be lowered to achieve a higher CO conversion, though the reaction rate is

kinetically suppressed at low temperature. For the industrial processes, the WGS reaction is performed using two stage catalytic processes; i.e., a high temperature shift (HTS) and low temperature shift (LTS). The HTS is carried out with a Fe₂O₃–Cr₂O₃ catalyst at a high temperature range (583–723 K) [4–6], and the LTS is performed with a Cu/ZnO/Al₂O₃ catalyst for decreasing the CO level to less than 1% in the low temperature range (483–523 K) [7–15]. Recently, a variety of catalysts has been reported; a highly active Pd/K/Fe₂O₃ catalyst at the mild temperature of 573 K [16], an alkali-promoted Pt/SiO₂ catalyst for the low temperature shift [17] and sustainable Cu/Al₂O₃ catalyst for the daily start-up and shutdown (DSS) like operation [18]. In addition, nano-sized gold has emerged as a prominent catalyst for the WGS reaction after the pioneering work of Haruta et al. [19], and a multitude of studies for an effective Au catalyst has been performed, such as the novel Au/La₂O₃ and Au/La₂O₂SO₄, Au/Fe₂O₃ and Au/CeO₂ as promising low-temperature shift catalysts [20–22]. However, the price of precious metals has increased every year. In terms of the cost for precious metals, a more efficient and low-cost catalyst needed to be developed.

* Corresponding author.

E-mail address: tcfukuh@ipc.shizuoka.ac.jp (C. Fukuhara).



Scheme 1. Preparation of the structured LaCoO₃ catalyst.

A preliminary study showed that the reduction temperature of the catalyst could influence the catalytic performance of the WGS reaction [23,24]. A precious metal supported on a perovskite-type oxide has the unique property; the reduction temperature of the perovskite-type oxide is significantly reduced by supporting novel metals such as platinum (Pt) and palladium (Pd). The reduction by the loading of Pd or Pt resulted in an increased of WGS reaction activity, in other words, the easier release of lattice oxygen, more CO was oxidized to CO₂ by the lattice oxygen in the LaCoO₃, and also accompanied by a change in the produced hydrogen. The mobility of the lattice oxygen in the catalyst was found to be a key point for achieving a high activity.

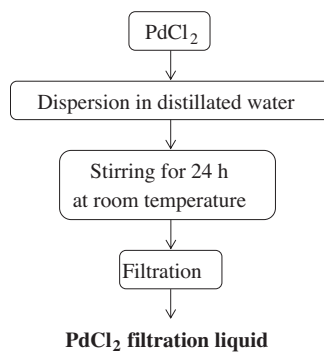
For the application for the perovskite-type catalyst to a fixed-bed reaction system, the lattice oxygen in the catalyst at the center of the reactor is not effectively utilized, compared to the catalyst in the vicinity of the reaction wall because a severe temperature gradient is generated from the reactor wall toward the center. For effectively utilizing the lattice oxygen in the catalyst, we focused on a plate type catalyst on a metal substrate [25–27]. The plate type catalyst, which is commonly called a structured catalyst, is composed of a regularly arranged catalyst on the metal plate. By placing the catalyst on the metal plate, an effective heat transfer to the reaction field could be achieved due to the conductional heat transfer. Furthermore, such a catalyst could overcome the disadvantage of a poor heat conductivity of the perovskite-type oxides, and high mobility of the lattice oxygen would be acquired at a low temperature due to the effective utilization for the external heat energy.

In this study, a plate-like LaCoO₃ catalyst was developed on the metal substrate by the following procedures; a viscous perovskite precursor solution was coated on a stainless steel substrate, then the coated substrate was calcined several times. The WGS performance of the plate-like LaCoO₃ catalyst was then investigated. Furthermore, for enhancing the WGS activity, the effects of Pd supported on the structured LaCoO₃ catalyst were examined by changing the types of Pd precursors.

2. Experimental

2.1. Preparation of the structured LaCoO₃ catalyst

Scheme 1 shows steps in the preparation of the structured LaCoO₃ catalyst. The preparation procedure of the catalyst was as



Scheme 2. Preparation of PdCl₂ filtration liquid.

follows: metal ion nitrates included in the perovskite type oxide were dissolved in distilled water, then citric acid was added to the solution at the 1/3 molar ratio of total metal ions/citric acid. It was then evaporated to form a powder at 353 K for 10 h. Following that, the powder was dissolved in H₂O again and a viscous gel solution was obtained. The adherence of the perovskite-type oxide onto the star-shaped metal substrate (20 mmφ × 30 mm length) was carried out by immersion of the substrate in the viscous gel solution. The metal substrate was stainless steel with a 100 μm thickness. After the gel coating, calcination of the coated substrate was performed at 673 K for 2 h. Finally, the substrate was calcined at 873 K for 10 h. The prepared catalyst in this way was represented as the structured LaCoO₃ catalyst.

2.2. Loading method of Pd on the structured LaCoO₃ catalyst

The Pd loading was performed by immersing the structured LaCoO₃ catalyst in an aqueous solution of the Pd precursor salt of Pd(NH₃)₄Cl₂ or Pd(ethylenediamine)₂Cl₂ (denoted as Pd(en)₂Cl₂) for 2 min. The Pd-dipped catalyst was then dried at room temperature for 30 min. These operations were repeated until a 1 wt% Pd loading was achieved. In addition, Pd(acetylacetone)₂ (denoted as Pd(acac)₂), which was dissolved in an acetone solution, was used as the precursor. PdCl₂ was also used as the precursor, however, the PdCl₂ hardly dissolved in the H₂O and organic solvents, unlike the other reagents. Therefore, a solution with a trace amount of the Pd component dissolved in H₂O was utilized as the precursor. Namely, the PdCl₂ reagent was dispersed in H₂O (denoted as the slurry) and the slurry was stirred for 24 h at room temperature. Filtration of the slurry was then performed, and the filtration liquid was used as the Pd precursor solution. **Scheme 2** shows steps in the preparation of this PdCl₂ filtration liquid. The pH of this filtration liquid was 2.5. After the Pd loading, the substrate was calcined at 823 K for 2 h.

The washing procedures for the highly active catalyst were applied in order to remove the chloride ligand from the Pd complexes loaded on the support. The washing agents were water, an aqueous solution of NH₃ or NaOH at pH 11.5. The washing procedure was employed by immersion of the Pd-supporting structured catalyst without calcination in each solution for 30 min without stirring. After immersion in each solution, the structured catalyst was washed with distilled water for 2 min. The catalyst was then calcined at 823 K for 2 h.

2.3. WGS performance

The WGS performance test of the prepared catalyst was performed at 573 K in a conventional flow reactor system. After setting the prepared catalyst in the reactor, the reactants of CO and H₂O were supplied at 12.2 and 24.4 ml min⁻¹, respectively. The ratio of

steam to carbon was 2. The catalyst weight was 0.5 g excluding the substrate weight. The gaseous reactants and products, such as CO, CO₂ and CH₄, after the trapping of steam in the effluent gas through the cold trap were collected by a gas-tight syringe, then injected into the off-line thermal conductivity detection gas chromatograph (GC-8A; Shimadzu Co., Ltd., Japan). After sampling at 10 min for the first plot, subsequent samplings were carried out every 20 min. The CO conversion and CO₂ selectivity were evaluated using Eqs. (2) and (3), in which [CO], [CO₂] and [CH₄] denote the concentration of CO, CO₂ and CH₄ in the outlet gas from the reactor. The carbon balances of these investigations amounted to ≥98%.

$$\text{CO conversion (\%)} = \frac{[\text{CO}_2] + [\text{CH}_4]}{[\text{CO}] + [\text{CO}_2] + [\text{CH}_4]} \times 100 \quad (2)$$

$$\text{CO}_2 \text{ selectivity (\%)} = \frac{[\text{CO}_2]}{[\text{CO}_2] + [\text{CH}_4]} \times 100 \quad (3)$$

2.4. Characterization of LaCoO₃ catalysts and Pd precursors

The crystalline structure of the catalyst was obtained by an XRD analysis (40 kV, 40 mA) using a X-ray diffraction meter (RINT-2200, Rigaku Co., Ltd.) and CuK α radiation source filtered by Ni. The surface structural properties of the catalyst were analyzed by Field Emission-Scanning Electron Microscope (JSM-7001F, JEOL Co., Ltd.) equipped with EDX and by a High Resolution-Transmission Electron Microscope (JEM-2010, JEOL Co., Ltd.).

The H₂-temperature-programmed-reduction (H₂-TPR) measurements were performed by a TAPS3000S (Bruker AXS Co., Ltd.). The catalyst sample (20 mg) was placed in the center of the muffle. The heating rate was 10 K min⁻¹ from 323 to 873 K. The weight loss of zero was defined as the starting weight of the catalyst at 323 K.

UV-vis spectroscopy measurements for clarifying the Pd species in the filtration liquid of the PdCl₂ slurry were carried out at room temperature by a UV-vis instrument (UV-1700, Shimadzu Co., Ltd.) in the range of 190–550 nm. Scans were performed with a data interval of 1 nm and a scan rate of 90 nm min⁻¹.

An X-ray photoelectron spectroscopy (XPS, ESCA-3400; Shimadzu Co., Ltd.) measurement was also performed using non-monochromatic AlK α radiation. The pass energy of the analyzer was at 23.5 eV. Binding energy of C1s at 284.7 eV was used for calibration.

3. Results and discussion

3.1. Morphology of the structured LaCoO₃ catalyst

Fig. 1 represents the XRD pattern of the as-made catalyst which was peeled off the stainless steel substrate. The peaks of the as-made catalyst corresponded to the perovskite structure of LaCoO₃ and no impurity phases were detected. For calculating the crystallite sizes using the Scherrer equation and the peak at $2\theta = 32.9^\circ$, the diameter was estimated to be 15.2 nm. This value was close to that in the literature [28,29]. **Fig. 2(a)** and (b) shows SEM images of the surface and cross section of the catalyst, including the results of the elemental analyses by EDX. As shown in **Fig. 2(a)**, the catalyst surface was composed of sintered spherical particles of 50 nm diameter that produced a porous-like structure. From the cross sectional view in **Fig. 2(b)**, the thickness of the formed layer, which was composed of La, Co and O elements, was about 20 μm . Based on these results, a LaCoO₃ catalyst layer was uniformly formed on the stainless steel substrate. In addition, the pores, which were observed on the LaCoO₃ surface as shown in **Fig. 2(a)**, were considered not to reach the substrate surface.

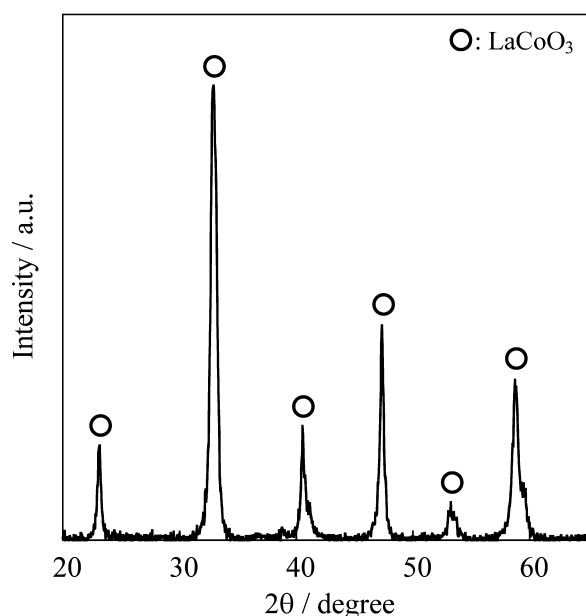


Fig. 1. XRD pattern of the coated catalyst component peeled off the stainless steel substrate.

3.2. WGS performance of structured LaCoO₃ and Pd supported catalyst

In order to evaluate the catalytic performance of the structured LaCoO₃ catalyst, the WGS reaction was carried out in the reaction temperature range of 523–873 K. **Fig. 3** represents the CO conversion as a function of the reaction temperatures. The catalytic activity over the structured LaCoO₃ catalyst increased with a change in the reaction temperature as follows; 0.7% at 523 K, 3.9% at 573 K, 14.7% at 623 K, 39.9% at 673 K, 64.5% at 723 K and 78.3% at 773 K. Although CH₄ was also produced as a by-product, the selectivity of CH₄ was less than 0.3% within the reaction temperature range from 523 to 873 K. The structured LaCoO₃ catalyst was a highly active and selective catalyst for the WGS reaction at high temperature, but the activity was not significantly high at the low temperatures from 523 to 573 K.

The loading of a precious metal promoted the ability of releasing the lattice oxygen, and such promotion resulted in an increased WGS performance [23,24]. In order to enhance the WGS activity of the structured catalyst, the LaCoO₃ catalyst supported Pd component was prepared and was its performance investigated. **Table 1** shows the CO conversion and selectivity to CO₂ and CH₄ at the time when a stable activity was obtained over the Pd-supported catalysts prepared using various palladium precursors. The CO conversion

Table 1

CO conversion and selectivity over the Pd/LaCoO₃ catalysts prepared with different types of palladium precursors.

Pd precursor	CO conversion/%	Selectivity/%	
		CO ₂	CH ₄
Pd(acac) ₂	20.3	99.4	0.6
Pd(NH ₃) ₄ Cl ₂	12.1	93.3	6.7
Pd(en) ₂ Cl ₂	13.2	99.8	0.2
PdCl ₂ filtrate	58.6	98.3	1.7
Bare LaCoO ₃	0.3	100.0	0.0
Pd/Al ₂ O ₃ ^a	1.0	100.0	0.0

Reaction condition: CO and H₂O were supplied at 12.2 and 24.4 ml min⁻¹, respectively; Catalyst weight was 0.5 g excluding the substrate weight; Reaction temperature was 573 K.

^a PdCl₂ filtrate was used as Pd precursor.

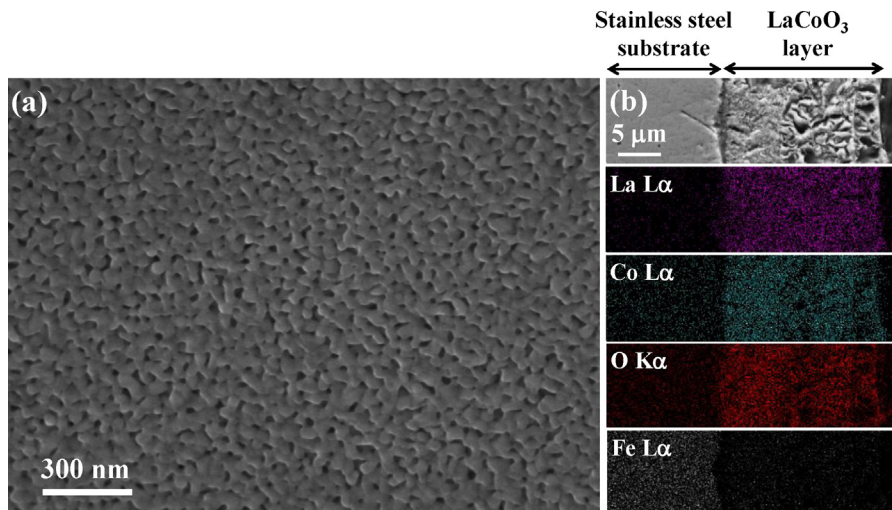


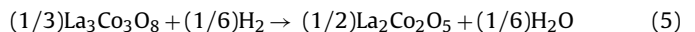
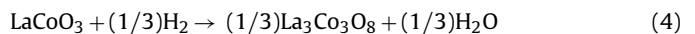
Fig. 2. SEM images and elemental analyses by EDX for (a) the surface and (b) the cross section of the structured LaCoO_3 catalyst.

was as follows: 20.3% over the catalyst prepared using $\text{Pd}(\text{acac})_2$, 12.1% over $\text{Pd}(\text{NH}_3)_4\text{Cl}_2$ and 13.2% over $\text{Pd}(\text{en})_2\text{Cl}_2$. However, when using the filtration liquid of the PdCl_2 slurry, a higher conversion of 58.6% was obtained. It was found that the types of Pd precursors seriously affected the WGS performance and the use of the filtration liquid was the most suitable. Since a Pd/ Al_2O_3 catalyst prepared using the filtration liquid and a bare LaCoO_3 catalyst showed a significantly low activity of 1.0% and 0.3% CO conversion at 573 K, as shown in Table 1, the activity progression by loading Pd would be due to a synergistic effect between the LaCoO_3 and the Pd component. In other words, the mobility of the lattice oxygen would be enhanced by the supported Pd on the LaCoO_3 and such progression might improve the WGS performance of the structured catalyst. Additionally, the CH_4 selectivity was only 1.7% over the Pd/ LaCoO_3 catalyst prepared using the PdCl_2 filtration liquid. It was found that the Pd/ LaCoO_3 catalyst was highly selective for the WGS reaction.

3.3. Role of Pd for WGS reaction

For clarifying the promotion by the supported Pd, H₂-TPR measurements were performed over the bare LaCoO_3 , the as-made Pd/ LaCoO_3 and the Pd/ LaCoO_3 after the WGS reaction (denoted as spent catalyst). Fig. 4 shows the reduction behavior of these

catalysts. The left axis denotes the weight loss and the right axis represents the differential value of the weight loss (Δ weight loss) which was obtained by dividing the weight loss by the temperature. From Fig. 4, a two-step reduction over the bare LaCoO_3 was observed at 654 and 837 K, which was known to occur; LaCoO_3 was reduced to $\text{LaCoO}_{2.5}$ ($1/2\text{La}_2\text{O}_3 + \text{CoO}$) corresponding to the Co^{3+} reduction to Co^{2+} at about 654 K, followed by $\text{LaCoO}_{2.5}$ being reduced to $\text{LaCoO}_{1.5}$ ($1/2\text{La}_2\text{O}_3 + \text{Co}$) corresponding to the Co^{2+} reduction to Co^0 at about 837 K. By supporting the Pd component, the reducibility of the Co cation was enhanced as shown in Fig. 4. The as-made Pd/ LaCoO_3 catalyst has three peaks at 386, 461 and 809 K as confirmed by the Δ weight loss, although the bare LaCoO_3 catalyst has two peaks at a higher temperature. Chiarello et al. reported that loading Pd promoted the reduction of the Co cation in LaCoO_3 , and Co^{3+} to Co^{2+} was reduced in two steps [30]. The two-step reduction was explained by Eqs. (4) and (5) on the catalyst:



They also found that these reactions progressed by incorporation of Pd as the B-site in LaCoO_3 . Due to the incorporation of

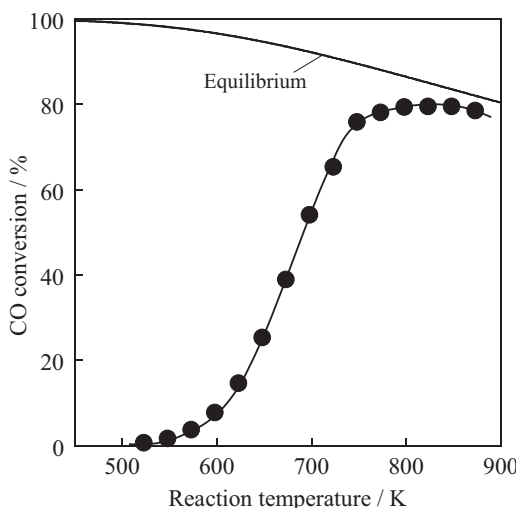


Fig. 3. CO conversion over the structured LaCoO_3 catalyst.

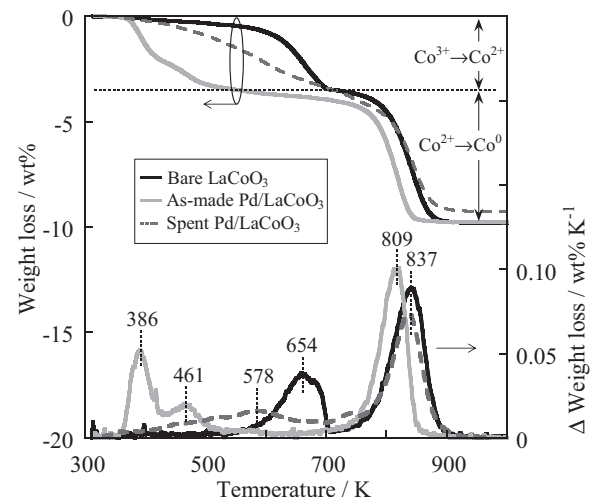


Fig. 4. Reduction behaviors in presence of H_2 over the bare LaCoO_3 , the as-made Pd/ LaCoO_3 and the spent Pd/ LaCoO_3 catalyst.

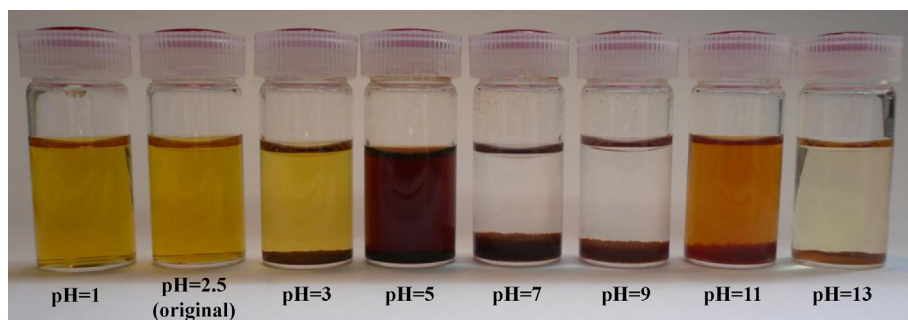


Fig. 5. Overview of the filtration liquids with different pH values.

Pd, the reduction of LaCoO_3 occurred through the intermediate phases with the general formula $\text{La}_n\text{Co}_n\text{O}_{3n-1}$. The initial and second reduction steps corresponded to $n=3$ (Eq. (4)) and 2 (Eq. (5)), respectively. From Fig. 4, the two-step reduction of Co^{3+} to Co^{2+} was confirmed over the as-made Pd/ LaCoO_3 catalyst as stated by Chiarello. Therefore, the supported Pd might be initially incorporated into the B-site of the LaCoO_3 .

On the other hands, the spent catalyst did not show a two-step reduction, but one moderate reduction at about 578 K was observed. The reason for the one moderate reduction might be derived from no-interaction of Pd with the bulk Co^{3+} in the perovskite structure because the Pd originally incorporated into the B-site appeared on the surface during the WGS reaction. Such surface Pd clusters triggered the dissociative adsorption of H_2 , and H adatoms were subsequently formed. The H adatoms lead to the consumption of the lattice oxygen at a lower reduction temperature as compared to the bare LaCoO_3 . Such a reduction promotion, which meant improvement of the releasing ability of the lattice oxygen, might improve the WGS performance. A preliminary study showed that the reaction mechanism of the WGS reaction was Mars van Krevelen using lattice oxygen by Eqs. (6) and (7) [24]:



In these equations, $\text{O}^{2-}_{\text{lat}}$ and V_{ox} denote the lattice oxygen and lattice vacancy in the catalyst, respectively. The key point of the WGS performance enhancement was improvement of the mobility of the lattice oxygen. Hence, the supported Pd produced a high mobility of the lattice oxygen and enhanced the WGS performance.

In addition, as shown in Fig. 4, a smaller weight loss was observed over the spent catalyst as compared to the as-made Pd/ LaCoO_3 . The imbalance of the release rate (Eq. (6)) and the regeneration rate of the lattice oxygen (Eq. (7)) was considered to produce a lattice vacancy in LaCoO_3 . In other words, the release rate of the lattice oxygen was higher than its regeneration rate. Therefore, the lattice oxygen diffused from the bulk to the surface of the LaCoO_3 catalyst, and a lattice vacancy was subsequently produced.

The synergistic effect as already mentioned could be controlled by changing the pH of the filtration liquid. Excluding pH = 2.5, the adjustment of the filtration liquid pH was carried out by adding NaOH *aq.* or HNO_3 *aq.* to the original filtration liquid. Fig. 5 shows a photograph of the filtration liquids with different pHs. By increasing the pH of the filtration liquid from 2.5 to 9, precipitation of the Pd component was found to proceed in the solution. On the other hand, when the pH further increased from 9 to 13, the precipitated Pd component was dissolved again. The Pd-supporting structured catalyst was prepared with these solutions, and the activity test was performed. Fig. 6 shows the CO conversion over the catalysts using the filtrate of pH = 1, 2.5 (the original filtration liquid), 3, 5, 7, 9, 11 and 13. The result showed that the CO conversion over these

catalysts at a steady-state was as follows; 19.5% (99.5%) for pH = 1, 65.9% (98.3%) for pH = 2.5, 61.7% (98.2%) for pH = 3, 16.2% (100%) for pH = 5, 3.2% (100%) for pH = 7, 2.9% (100%) for pH = 9, 2.7% (100%) for pH = 11 and 22.0% (99.8%) for pH = 13. The value in parenthesis was the selectivity for CO_2 , which was not shown in Fig. 6. The selectivity for CO_2 was almost the same over these catalysts. In terms of the activity, the optimum pH value of the filtration liquid was 2.5 for producing a high WGS performance. The reason for such an optimization will be discussed in the next section.

3.4. Relationship between WGS performance and Pd state of the filtration liquid

For elucidating the reason for the high performance obtained over the catalyst prepared using the filtration liquid of PdCl_2 , TEM measurements were carried out. Fig. 7(a) and (b) shows TEM images of the as-made and the spent Pd/ LaCoO_3 catalyst, respectively. Here, the spent catalyst denotes the catalyst after a 190-min WGS reaction. In Fig. 7(a), the Pd species were not clearly determined. The size of Pd on the as-made catalyst might be less than 1 nm, or Pd might be incorporated into the B-site of the LaCoO_3 . As for the spent catalyst in Fig. 7(b), there was a portion indicated by the arrow whose color was darker than the LaCoO_3 layer. The supported Pd might be the darker portion because heavier elements such as Pd appeared darker due to scattering of the electrons in the catalyst in the TEM measurements. The supported Pd was sintered during the reaction and its particle size grew to about 2–5 nm. Although the

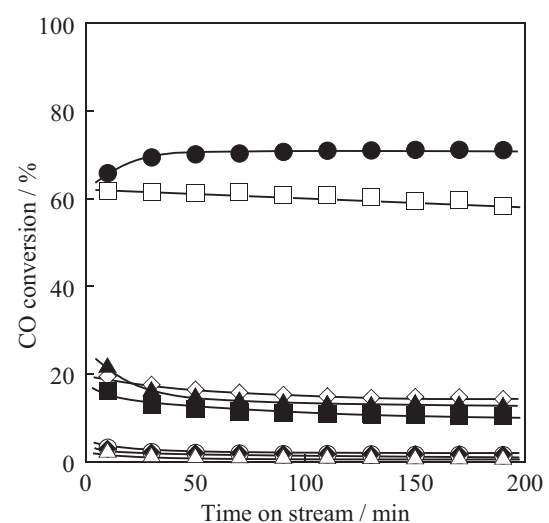


Fig. 6. Effect of pH of the filtration liquid on CO conversion at 573 K: (◊) pH = 1, (●) pH = 2.5 (original), (□) pH = 3, (■) pH = 5, (○) pH = 7, (◆) pH = 9, (△) pH = 11 and (▲) pH = 13.

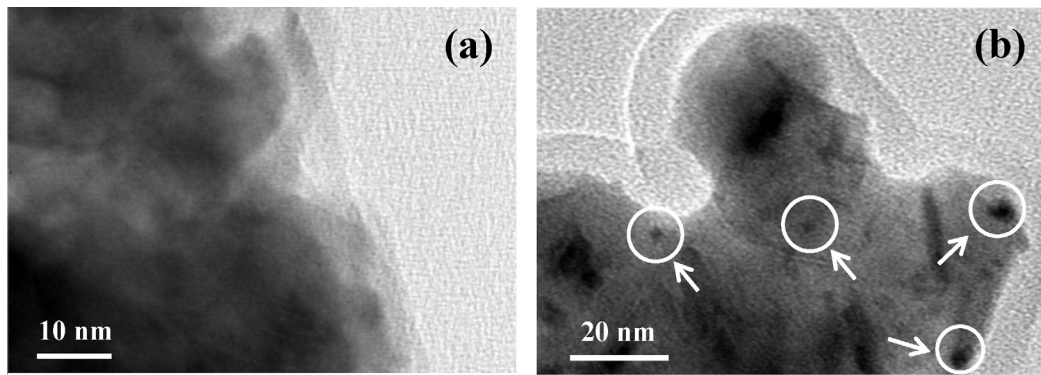
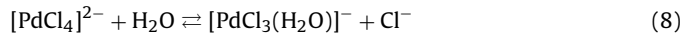


Fig. 7. TEM images of (a) the as-made Pd/LaCoO₃ catalyst and (b) the spent Pd/LaCoO₃ catalyst.

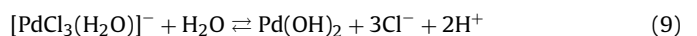
particle growth proceeded, the particle size was found to be quite small after the reaction. For investigating the advantage of the proposed method, we compared the different catalysts prepared by the impregnation method. Supporting data 1 shows TEM images of the as-made catalyst prepared by the impregnation method. In supporting data 1, particles indicated by the arrow were considered to be Pd. Its diameter was larger than 6 nm. Comparing the particle size of the catalyst prepared with the filtration liquid to that of the catalyst prepared by the impregnation method, the smaller Pd was obtained over the catalyst prepared with the filtration liquid. This proposed method using the filtration method had the advantage of Pd particle size.

The Pd species in the filtration liquid was identified by a UV-vis measurement. Fig. 8 shows the UV-vis spectra of the original filtration liquid and the solutions after several dip-coatings. From Fig. 8, two peaks at 210 and 238 nm were observed, and these peaks were found to decrease with the change in number of dip-coatings. These two peaks were assigned to the complex of the [PdCl₃(H₂O)][−] [31]. The decrease in the absorption peaks in the spectrum is due to the decrease in the [PdCl₃(H₂O)][−] concentration of the solution. Namely, the [PdCl₃(H₂O)][−] was loaded on the structured LaCoO₃ catalyst. The PdCl₂ is known to be hardly dissolved in H₂O, however, a trace amount of Pd was dissolved as [PdCl₄]^{2−}, [PdCl₃(H₂O)][−] and PdCl₂(H₂O)₂. Also, the state of Pd was dependent on the concentration of the chloride ion and proton in the solution [32]. As shown in Fig. 8, only the [PdCl₃(H₂O)][−] species was observed in the filtration liquid in this study. The following reaction (Eq. (8)) proceeded

in the filtrate after a trace amount of PdCl₂ was dissolved in the solution as [PdCl₄]^{2−} [33].



By the way, the pH of the filtrate of the PdCl₂ slurry was 2.5. Braisted et al. reported that the LaCoO₃ support surface carried a net positive charge in the solution at a low pH [34]. Therefore, the Pd loading on the support surface was considered to be driven by an electrostatic interaction between the anionic charged precursor of [PdCl₃(H₂O)][−] and the oppositely charged support surface. The electrostatic interaction might produce highly dispersed Pd on the structured catalyst. Table 2 shows the concentrations of the [PdCl₃(H₂O)][−] in the filtrate of the PdCl₂ slurry and after the dip-coating (2 min, 5 times) on the structured LaCoO₃ catalyst which were measured by ICP. The concentration of the as-made filtrate was 793 ppm, on the other hand, the concentration of the filtrate after the dip-coating was 589 ppm. The decrease in the concentration of [PdCl₃(H₂O)][−] proceeded by only immersing the structured catalyst in the filtration liquid, which was due to the electrostatic interaction between the Pd precursor and the support. The reason for the optimum pH of the Pd precursor solution was considered to be derived from the Pd state in the precursor solution. It was reported that a Pd(OH)₂ species precipitated by increasing the pH of the filtration liquid as noted by the following reaction (Eq. (9)) [33].



There was no electrostatic interaction between Pd(OH)₂ and the cationically charged support surface, which might lead to a low Pd dispersion state. It might cause a significantly lower activity over the catalyst prepared using the filtrate at a pH of more than 3. In addition, the low CO conversion when pH=1 might be due to the chloride ion in the Pd precursor solution. The solution (pH=1) was prepared from the original Pd precursor solution (pH=2.5) by adjusting with HCl. Namely, the chloride ion was more contained in the solution (pH=1). To confirm the effect of the chloride ion on the catalytic performance, the Pd solution, which nearly 4-fold chloride ion was contained in, was prepared. The prepared catalyst was denoted as the Pd/LaCoO₃ (Cl excess). Supporting data 2 shows the CO conversion over the Pd/LaCoO₃ catalyst prepared with the filtration liquid, which

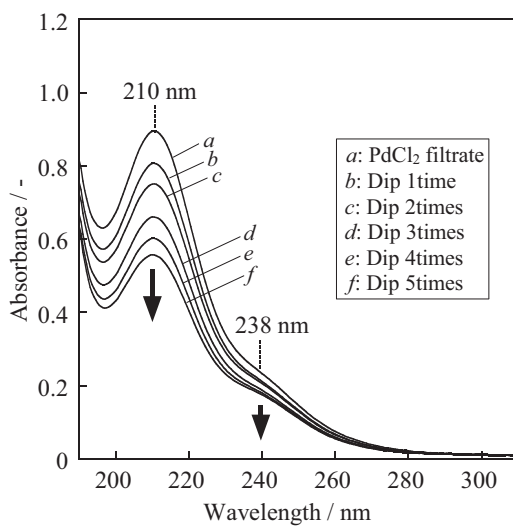


Fig. 8. UV-vis spectra of the PdCl₂ filtrate and solutions after the dip-coating.

Table 2

Concentration of the [PdCl₃(H₂O)][−] in the filtrate of the PdCl₂ slurry and after the dip-coating.

Condition	Concentration/ppm
As-made filtrate	793
Filtrate after 5 dippings for 2 min	589

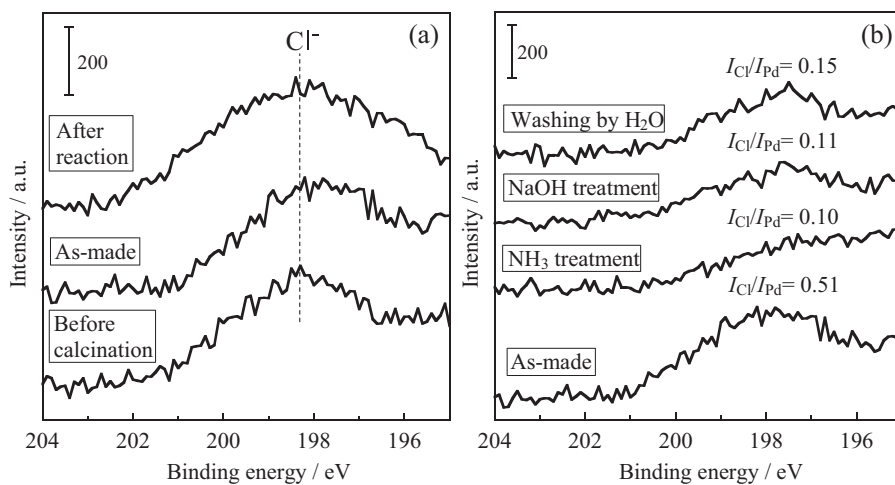


Fig. 9. XPS spectra of $\text{Cl}_{2\text{p}}$ for the Pd/LaCoO_3 catalyst (a) in each step and (b) with washing treatment by basic solution and/or water.

was abbreviated as the Pd/LaCoO_3 (original), and the Pd/LaCoO_3 (Cl excess) catalyst. The CO conversion at a steady-state was 65.9% for the Pd/LaCoO_3 (original) catalyst and 6.6% for the Pd/LaCoO_3 (Cl excess) catalyst. Such a result indicated that the chloride ion inhibited the catalytic activity for WGS reaction. The activity suppression by chloride ion was reported by other researchers. Oh et al. reported that the dual role of Cl^- in suppressing the CO preferential oxidation ($\text{CO} + 1/2\text{O}_2 \rightarrow \text{CO}_2$) activity over the $\text{Au}/\text{Al}_2\text{O}_3$ catalyst was accelerating the agglomeration of Au particles and poisoning the active sites [35]. The work of Lin et al. suggested that the low catalytic activities for CO oxidation in the Au/TiO_2 catalyst with high chloride contents may also be due to an inhibitive effect [36]. They prepared catalysts by introducing AuCl_3 on TiO_2 using the incipient wetness method and observed that the activity for the Au/TiO_2 reduced with H_2 at 500 °C was 40-fold higher than those reduced at 200 °C. The improvement in catalytic property was accompanied by a threefold decrease in the residual Cl^- content of the catalyst but no significant change in the particle size of Au. In our results, the residual Cl^- had the impact on the catalytic properties, which might be due to the poisoning the active sites. The low CO conversion when pH = 1 would be due to the chloride ion in the Pd precursor solution.

3.5. Effect of post-treatment of the Pd-supported catalyst on performance

The $[\text{PdCl}_3(\text{H}_2\text{O})]^-$ of the Pd precursor contains chloride ions in its Pd complex. Generally, the presence of chloride ions causes a metal particle growth and deactivates the active site for the CO adsorption [35,37]. The XPS spectra of $\text{Cl}_{2\text{p}}$ over the Pd/LaCoO_3 catalyst before calcination, as-made and after the reaction were collected for elucidating whether or not chloride ions were present. Fig. 9(a) shows the XPS spectra of these catalysts. Surface chloride ion was detected over these catalysts. The chloride ion remained and seemed not to be affected by the thermal treatment on the support surface, although the calcination was performed at the high temperature of 823 K for 2 h to eliminate the chloride ion on the support surface. Xu et al. reported that the remaining chlorine on the catalyst surface could be removed by washing [38]. A washing procedure was then applied to remove the chloride ligands from the $[\text{PdCl}_3(\text{H}_2\text{O})]^-$. For the chloride removal, a washing procedure by a basic agent was performed because the presence of a basic agent would permit the substitution of the chloride ions by hydroxyl groups. The washing agents were aqueous solutions of NH_3 and NaOH . Additionally, the effect of washing with water was also examined. Fig. 9(b) shows the $\text{Cl}_{2\text{p}}$ XPS spectra of the untreated

and treated catalysts. From Fig. 9(b), the chloride ion was detected and the remaining chloride ion of the as-made catalyst was partially eliminated on the support surface, based on the decline of the $\text{Cl}_{2\text{p}}$ peak intensity. From the XPS spectra of $\text{Pd}_{3\text{d}}$ over the untreated and treated catalysts, Pd was confirmed to be the divalent state as shown in supporting data 3. The $\text{Pd}_{3d5/2}$ and $\text{Pd}_{3d3/2}$ spin-orbital splitting photoelectrons for these catalysts were located at binding energies of 336.9 and 342.4 eV, which were assigned to Pd^{2+} . For evaluating whether or not the chloride ion was eliminated, the ratio of the intensity for $\text{Cl}_{2\text{p}}$ - to $\text{Pd}_{3\text{d}}$ -level photoelectron peaks ($I_{\text{Cl}}/I_{\text{Pd}}$), which reflected the atomic ratio of Cl to Pd elements on the surface layers, was calculated. These values are also shown in Fig. 9(b). The values of $I_{\text{Cl}}/I_{\text{Pd}}$ were 0.51 for the catalyst without treatment, 0.10 for the NH_3 -treated catalyst, 0.11 for the NaOH -treated catalyst and 0.15 for the water-washed catalyst. The water or base treatment was found to be effective for elimination of the chloride ion on the catalyst.

Fig. 10 shows the CO conversion over the untreated catalyst and the treated catalysts. The value in parentheses is the CO_2 selectivity at a steady-state. The product except for CO_2 was CH_4 over the untreated and the treated catalysts. By washing the Pd-supported catalyst, the CO conversion was improved as follows: 83.6% at 10 min for washing with water; 82.0% for the NH_3 and 85.4% for

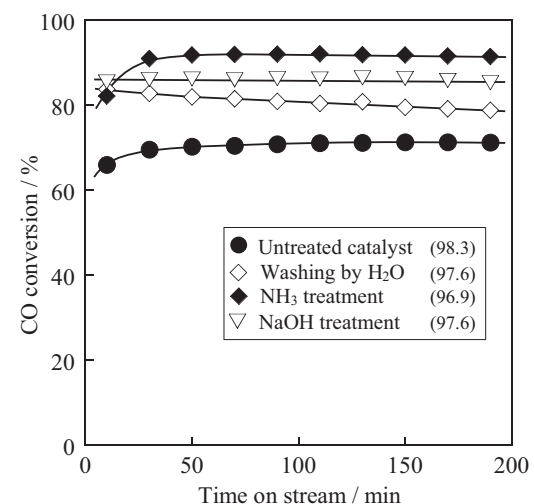


Fig. 10. CO conversion over the Pd/LaCoO_3 structured catalysts: (●) untreated, (○) with H_2O washing, (▽) with NaOH *aq.* washing (pH = 11.5), (◆) with NH_3 *aq.* washing (pH = 11.5).

the NaOH. Especially, the CO conversion over the NH₃-treated catalyst increased with time on stream and a 91.3% conversion was obtained at 190 min. Post-treatment by NH₃ was the most effective for improvement of the WGS activity. The CO₂ selectivity over the treated catalysts was as follows; 96.9% over the NH₃-treated catalyst, 97.6% over the NaOH-treated catalyst and 97.6% over the water-washed catalyst. Compared with the CO₂ selectivity of 98.3% over the untreated structured catalyst, the treated catalyst showed a slightly lower selectivity. Such a slightly lower selectivity was due to the production of methane which was produced from the unreacted CO and the produced hydrogen. Although a trace amount of chloride ion remained on the support surface, the washing process had a positive effect for further improving the WGS performance over the Pd-supported structured catalyst.

In summary, the structured LaCoO₃ catalyst prepared with utilizing a singular precursor of [PdCl₃(H₂O)][−] showed high performance for the WGS reaction. Additionally, the Pd loading method was a very simple, which was only dipping in the precursor solution with a few times, and the resulting Pd particle size was a quite small. Further enhancement of the catalytic performance would be expected by the optimization of washing treatment with NH₃ for eliminating the chloride ligand. Its simple dip-coating method and washing procedure might contribute to the effective loading of active metals on the structured catalyst.

4. Conclusion

The novel structured LaCoO₃ perovskite-type catalyst was developed for effectively converting CO via the WGS reaction. Among the various Pd-supported LaCoO₃ catalysts, the catalyst prepared by the filtration liquid of the PdCl₂ slurry showed the highest activity. High activity was due to the electrostatic interaction between [PdCl₃(H₂O)][−] as the anionic charged precursor and the oppositely charged LaCoO₃ support surface, which produced highly dispersed state of Pd on the support. For removing the chloride ligand from the [PdCl₃(H₂O)][−], washing procedures of the Pd supported catalyst were applied using water, NH₃ and NaOH. Consequently, the catalytic performance was improved by all washing processes. Especially, the post-treatment by NH₃ was the most effective for improvement of WGS performance.

Acknowledgement

This work was supported in part by JST, A-Step (AS242Z02697M). We greatly thank Prof. Shigeki Tsukui (Osaka Prefecture University) for ICP measurement.

Appendix A. Supplementary data

Supplementary data associated with this article can be found, in the online version, at <http://dx.doi.org/10.1016/j.apcata.2014.03.005>.

References

- [1] S. Ahmed, M. Krumpelt, Int. J. Hydrogen Energy 26 (2001) 291–301.
- [2] G.G. Scherer, Solid State Ionics 94 (1997) 249–257.
- [3] T.V. Choudhary, D.W. Goodman, Catal. Today 77 (2002) 65–78.
- [4] S. Oki, R. Mezaki, J. Phys. Chem. 77 (1973) 1601–1605.
- [5] S. Oki, R. Mezaki, Ind. Eng. Chem. Res. 27 (1988) 15–21.
- [6] M. Tinkle, J.A. Dumesic, J. Catal. 103 (1987) 65–78.
- [7] C. Rhodes, B.P. Williams, F. King, G.J. Hutchings, Catal. Commun. 3 (2002) 381–384.
- [8] Y. Lei, N.W. Cant, D.L. Trimm, J. Catal. 239 (2006) 227–236.
- [9] A.F. Ghenciu, Curr. Opin. Solid State Mater. Sci. 6 (2002) 389–399.
- [10] M.J.L. Ginés, N. Amadeo, M. Laborde, C.R. Apesteguía, Appl. Catal. A: Gen. 131 (1995) 283–296.
- [11] O. Ilinich, W. Ruetttinger, X. Liu, R. Farrauto, J. Catal. 247 (2007) 112–118.
- [12] P.J. Guo, L.F. Chen, G.B. Yu, Y. Zhu, M.H. Qiao, H.L. Xu, K.N. Fan, Catal. Commun. 10 (2009) 1252–1256.
- [13] T. Shishido, M. Yamamoto, D. Li, Y. Tian, H. Morioka, M. Honda, T. Sano, K. Takehira, Appl. Catal. A: Gen. 303 (2006) 62–71.
- [14] T. Shishido, M. Yamamoto, I. Atake, D. Li, Y. Tian, H. Morioka, M. Honda, T. Sano, K. Takehira, J. Mol. Catal. A: Chem. 253 (2006) 270–278.
- [15] H. Yahiro, K. Murawaki, K. Saiki, T. Yamamoto, H. Yamaura, Catal. Today 126 (2007) 436–440.
- [16] Y. Sekine, T. Chihara, R. Watanabe, Y. Sakamoto, M. Matsukata, E. Kikuchi, Catal. Lett. 140 (2010) 184–188.
- [17] Y. Zhai, D. Pierre, R. Si, W. Deng, P. Ferrin, A.U. Nilekar, G. Peng, J.A. Herron, D.C. Bell, H. Saltsburg, M. Mavrikakis, M. Flytzani-Stephanopoulos, Science 329 (2010) 1633–1636.
- [18] S. Nishimura, T. Shishido, K. Ebitani, K. Teramura, T. Tanaka, Appl. Catal. A 387 (2010) 185–194.
- [19] M. Haruta, S. Tsubota, T. Kobayashi, H. Kageyama, M.J. Genet, B. Delmon, J. Catal. 144 (1993) 175–192.
- [20] J.D. Lessard, I. Valsamakis, M. Flytzani-Stephanopoulos, Chem. Commun. 48 (2012) 4857–4859.
- [21] D. Andreeva, V. Idakiev, T. Tabakova, A. Andreev, J. Catal. 158 (1996) 354–355.
- [22] Q. Fu, A. Weber, M. Flytzani-Stephanopoulos, Catal. Lett. 77 (2001) 87–95.
- [23] Y. Sekine, H. Takamatsu, S. Aramaki, K. Ichishima, M. Takada, M. Matsukata, E. Kikuchi, Appl. Catal. A 352 (2009) 214–222.
- [24] R. Watanabe, Y. Sekine, H. Takamatsu, Y. Sakamoto, S. Aramaki, M. Matsukata, E. Kikuchi, Top. Catal. 53 (2010) 621–628.
- [25] C. Fukuhara, H. Ohkura, K. Gonohe, A. Igarashi, Appl. Catal. Gen. 279 (2005) 195–203.
- [26] C. Fukuhara, Y. Kamata, A. Igarashi, Appl. Catal. Gen. 330 (2007) 108–116.
- [27] V. Meille, Appl. Catal. Gen. 315 (2006) 1–17.
- [28] Y. Zhu, R. Tan, T. Yi, S. Ji, X. Ye, Li. Cao, J. Mater. Sci. 35 (2000) 5415–5420.
- [29] N. Yi, Y. Cao, Y. Su, W.-L. Dai, H.-Y. He, K.-N. Fan, J. Catal. 230 (2005) 249–253.
- [30] G.L. Chiarello, J.-D. Grunwaldt, D. Ferri, F. Krumeich, C. Oliva, L. Forni, A. Baiker, J. Catal. 252 (2007) 127–136.
- [31] C.T. Tait, D.R. Janecky, P.S.Z. Rogers, Geochim. Cosmochim. Acta 55 (1991) 1253–1264.
- [32] J.-F. Boily, T.M. Seward, Geochim. Cosmochim. Acta 69 (2005) 3773–3789.
- [33] O.B. Bel'skaya, T.I. Gulyaeva, A.B. Arbuzov, V.K. Duplyakin, V.A. Likholobov, Kinet. Catal. 51 (2010) 105–112.
- [34] M.P. Braisted, L.M. Cirjak, D.L. Feke, I. Manas-Zloczower, Part. Part. Syst. Charact. 23 (2006) 480–483.
- [35] H.-S. Oh, J.H. Yang, C.K. Costello, Y.M. Wang, S.R. Bare, H.H. Kung, M.C. Kung, J. Catal. 210 (2002) 375–386.
- [36] S.D. Lin, M. Bollinger, M.A. Vannice, Catal. Lett. 17 (1993) 245–262.
- [37] C.K. Costello, M.C. Kung, H.-S. Oh, Y. Wang, H.H. Kung, Appl. Catal. Gen. 232 (2002) 159–168.
- [38] Q. Xu, K.C.C. Kharas, A.K. Datye, Catal. Lett. 85 (2003) 229–235.